Probing the Role of Tyr 64 of *Treponema denticola* Cystalysin by Site-Directed Mutagenesis and Kinetic Studies†

Barbara Cellini,‡ Mariarita Bertoldi,‡ Riccardo Montioli, and Carla Borri Voltattorni*

Dipartimento di Scienze Neurologiche e della Visione, Sezione di Chimica Biologica, Facoltà di Medicina e Chirurgia, Università degli Studi di Verona, Strada Le Grazie, 8, 37134 Verona, Italy

Received July 21, 2005; Revised Manuscript Received August 20, 2005

ABSTRACT: Tyr 64, hydrogen-bonded to coenzyme phosphate in *Treponema denticola* cystalysin, was changed to alanine by site-directed mutagenesis. Spectroscopic and kinetic properties of the Tyr 64 mutant were investigated in an effort to explore the differences in coenzyme structure and kinetic mechanism relative to those of the wild-type enzyme. The wild type displays coenzyme absorbance bands at 418 and 320 nm, previously attributed to ketoenamine and substituted aldamine, respectively. The Tyr 64 mutant exhibits absorption maxima at 412 and 325 nm. However, the fluorescence characteristics of the latter band are consistent with its assignment to the enolimine form of the Schiff base. pK_{spec} values of ∼8.3 and ∼6.5 were observed in a pH titration of the wild-type and mutant coenzyme absorbances, respectively. Thus, Tyr 64 is probably the residue involved in the nucleophilic attack on C4′ of pyridoxal 5′-phosphate (PLP) in the internal aldimine. Although the Tyr 64 mutant exhibits a lower affinity for PLP and lower turnover numbers for α,β-elimination and racemization than the wild type, the pH profiles for their $K_{d(PLP)}$ and kinetic parameters are very similar. Rapid scanning stopped-flow and chemical quench experiments suggest that, in contrast to the wild type, for which the rate-determining step of α,β-elimination of β-chloro-L-alanine is the release of pyruvate, the rate-determining step for the mutant in the same reaction is the formation of α-aminoacrylate. Altogether, these results provide new insights into the catalytic mechanism of cystalysin and highlight the functional role of Tyr 64.

Cystalysin from *Treponema denticola* is a homodimeric pyridoxal 5′-phosphate (PLP[1])-dependent enzyme which catalyzes the α,β-elimination of L-cysteine to produce pyruvate, ammonia, and H_2S (*1*). Several sulfur- and non-sulfur-containing amino acids also serve as substrates for this reaction (*2*). Like other PLP enzymes, cystalysin is endowed with a high degree of catalytic versatility. Indeed, the enzyme catalyzes an alanine racemase reaction (*3*), the β-desulfination of L-cysteinesulfinic acid, and the β-decarboxylation of L-aspartate and oxalacetate (*4*) with turnover times measured in seconds. It also catalyzes with turnover times measured in minutes the overall transamination of both enantiomers of alanine (*3*). The pH dependencies of the kinetic parameters for the α,β-elimination and racemization reactions have been determined, and the pK_a's observed have been tentatively assigned to active site residues (*2, 3*). Additionally, site-directed mutagenesis studies have provided evidence that Lys 238, the PLP-binding lysine, is an essential residue for the α,β-elimination reaction catalyzed by cystalysin. In particular, we have proposed a triple role for Lys 238. This residue strengthens PLP binding and enhances the formation and dissociation of the enzyme and ligand Schiff bases, allowing more facile transimination. It also has a catalytic role, possibly participating as a general base abstracting the Cα proton from the substrate and as a general acid protonating the β-leaving group (*5*). There has been evidence of a two-base racemization mechanism of both enantiomers of alanine in which Lys 238 has been unequivocally identified as the catalyst acting on the *si* face, while Tyr 123 interacting with water molecules seems to be critical for an efficient proton abstraction/donation function on the *re* face (*6*).

The crystal structure of cystalysin, determined at 1.9 Å resolution, reveals tertiary and quaternary structures similar to those of aminotransferases (*7*). The PLP cofactor is bound in the center of each cystalysin monomer in a wide catalytic cleft. This crevice is formed by both the large PLP-binding domain and the small domain of one subunit and by the large domain from the neighboring subunit. The phosphate ester on C5′ is involved in multiple hydrogen bonds with either protein residues (Ser 237, Val 98, Val 99, and Tyr 64*) or two water molecules. Additional interactions are formed between amino acid residues and groups on the coenzyme (e.g., pyridine nitrogen and phenolic 3′-hydroxyl group). The interaction of the phosphate of PLP with a Gly-rich loop is a common feature of PLP enzymes of fold types I, II, and IV (*8*). Nevertheless, like in cystalysin, a tyrosyl residue has been found to be involved in the interaction with the PLP phosphate in aspartate aminotransferase (Tyr 70) (*9*, *10*), in tyrosine phenol lyase (Tyr 71) (*11*), in cystathionine β-lyase

† This work was supported by funding from the Italian Ministero dell'Università e Ricerca Scientifica e Tecnologica (to C.B.V.).

* To whom correspondence should be addressed: Dipartimento di Scienze Neurologiche e della Visione, sezione di Chimica Biologica, Strada Le Grazie, 8, 37134 Verona, Italy. Telephone: +39-045-8027-175. Fax: +39-045-8027-170. E-mail: carla.borrivoltattorni@univr.it.

‡ These authors contributed equally to this work.

[1] Abbreviations: PLP, pyridoxal 5′-phosphate; PMP, pyridoxamine 5′-phosphate; HPLC, high-pressure liquid chromatography.

10.1021/bi051433n CCC: $30.25
Published on Web 09/27/2005

(Tyr 111) (*12*), in tryptophan indole lyase (Tyr 72) (*13*), and in MalY (Tyr 61) (*14*). This residue's function appears to be different among the PLP enzymes examined so far. In tyrosine phenol lyase, Tyr 71 plays a critical role in both PLP binding and the β-elimination reaction (*11*), and Tyr 70 in aspartate aminotransferase has a function in stabilizing the holoenzyme complexes and in preventing the dissociation of the coenzyme from the enzyme molecule (*9*, *10*). On the other hand, the three-dimensional structures of cystathionine β-lyase (*12*) and cystalysin (*7*) suggest that Tyr 55 and Tyr 64 guide, respectively, the amino group of the PLP lysine to the substrate leaving group.

To investigate the role of Tyr 64 in the cystalysin mechanism, we have prepared the Y64A mutant and characterized its structural and functional properties. The results indicate that mutation of Tyr 64 not only weakens PLP binding but also alters its mode of binding and, consequently, the pH dependence of the coenzyme absorbance of wild-type cystalysin. The inability of the Tyr 64 mutant to form a substituted aldamine, the predominant form of the wild type at high pH, strongly suggests that Tyr 64 is the residue involved in the nucleophilic attack on C4′ of the coenzyme. In addition, the Tyr 64 mutant is seen to be 10−20-fold less active than the wild type, thus suggesting that Tyr 64 is not an essential residue for α,β-elimination and racemization. The wild-type and mutant pH−rate profiles, both measured at saturating PLP concentrations, are found to be very similar. Nevertheless, rapid scanning stopped-flow studies together with chemical quench experiments provide evidence that the rate-limiting step of the overall α,β-elimination reaction is the release of pyruvate for the wild type, while it is the release of the leaving group for the Y64A mutant.

EXPERIMENTAL PROCEDURES

Materials. PLP, β-chloro-L-alanine, L- and D-alanine, glycine, L-methionine, NAD^+ and NADH, pyruvate, rabbit muscle lactate dehydrogenase, alanine dehydrogenase in 50% glycerol, and D-amino acid oxidase were from Sigma. All other chemicals were of the highest grade commercially available. Bis-Tris-propane at a final concentration of 20 mM was used over the pH range of 5.8−9.2, and the ionic strength was kept constant by addition of KCl.

Site-Directed Mutagenesis. The Tyr 64 mutant form of cystalysin was made on the wild-type construct pUC18:*hly* (*1*) using the QuikChange site-directed mutagenesis kit from Strategene (La Jolla, CA). The kit employs double-strand DNA as a template, two complementary oligonucleotide primers containing the desired mutation, and *Dpn*I endonuclease to digest the parental DNA template. The oligonucleotide was synthesized by MWG-Biotech AG (Anzinger, Germany). The Tyr 64 mutant was produced using as a primer 5′ GACGAAACAGTGTTAGGAGCTACAGGACCTACTGAAGAG 3′ and its complementary oligonucleotide. The coding region of the mutated *hly* gene was sequenced to confirm the mutation. *Escherichia coli* strain DH5α cells were transformed and used for expression.

Expression and Purification of the Tyr 64 Mutant. The conditions used for expression and purification of the Tyr 64 mutant were as described for the wild-type enzyme (*2*). The protein concentration was determined by absorbance spectroscopy using a previously determined extinction coefficient of 12.77×10^4 M^{-1} cm^{-1} at 281 nm (*2*). The PLP content of wild-type and mutant enzymes was determined by releasing the coenzyme in 0.1 N NaOH and using an ϵ of 6600 M^{-1} cm^{-1} at 388 nm (*15*).

Preparation and Reconstitution of the Apo Form of the Tyr 64 Mutant. The apo form of the Tyr 64 mutant was prepared as previously reported for the wild type (*2*). For reconstitution, a 10-fold molar excess of PLP was added, and after 1 h, the solution was loaded on a desalting Hi-Prep 26/10 column previously equilibrated with 20 mM potassium phosphate buffer (pH 7.4). The enzyme was concentrated in microconcentrators. The apparent equilibrium constant for dissociation of PLP from the wild type and Tyr 64 mutant, $K_{d(PLP)}$, was determined by measuring either the α,β-eliminase activity of apoenzymes in the presence of PLP or the CD spectrometric titration of the apoenzymes with PLP. The apo forms of wild-type and mutant enzymes were in Bis-Tris-propane at the desired pH over a concentration range of 10−400 nM for enzymatic measurements and at 10 μM for CD measurements. A series of PLP stocks were prepared, and a minimum amount of each was added to the apoenzyme to achieve the desired PLP concentration. After incubation for 15 min, eliminase activity in the presence of β-chloro-L-alanine or CD spectra in the visible region were measured after each addition of PLP.

The $K_{d(PLP)}$ value of the enzyme−coenzyme complex was obtained according to eq 1:

$$Y = Y_{max}\{[E]_t + [PLP]_t + K_{d(PLP)} - \sqrt{([E]_t + [PLP]_t + K_d)^2 - 4[E]_t[PLP]_t}\}/\{2[E]_t\} \quad (1)$$

where $[E]_t$ and $[PLP]_t$ represent the total concentrations of cystalysin dimer and PLP, respectively, Y refers to the enzymatic activity or visible CD signal change at the PLP concentration, and Y_{max} refers to the enzymatic activity or CD signal when all enzyme molecules are complexed with the coenzyme.

Enzyme Activity Measurements. The α,β-elimination activity of cystalysin toward β-chloro-L-alanine was measured by the spectrophotometric assay coupled with lactate dehydrogenase as described previously (*2*). In the experiments designed to assess the formation of pyruvate during quench kinetic measurements, the level of production of pyruvate was determined by an assay based on measuring the amount of the dinitrophenylhydrazine derivative by high-performance liquid chromatography (HPLC) essentially as described by Neidle and Dunlop (*16*). The conversion of alanine in the L → D or D → L direction was measured using D-amino acid oxidase and lactate dehydrogenase or L-alanine dehydrogenase as the coupling enzymes, respectively, as reported previously (*3*). Aminotransferase activity was measured by monitoring either absorbance changes at 325 nm or the PMP formation as reported previously (*3*). To determine the kinetic parameters of the catalytic activities, the assays were performed as indicated above using a fixed amount of enzyme in the presence of exogenous PLP (100 and 400 μM for the wild type and mutant, respectively), where the substrate concentration was varied from 0.02 to 10 mM and from 0.15 to 500 mM for eliminase and racemase activities,

respectively. The experimental data were fit to the Michaelis−Menten equation to determine K_m and k_{cat} values.

Spectral Measurements. Absorption measurements were made with a Jasco V-550 spectrophotometer. The enzyme solution was drawn through a 0.2 μm filter to reduce light scattering from the small amount of precipitate. Fluorescence spectra were taken with a FP750 Jasco spectrofluorometer using 5 nm excitation and emission bandwidths at a protein concentration of 20 μM. Spectra of blanks, i.e., samples containing all components except cystalysin, were taken immediately before the measurements of samples containing protein. CD spectra were obtained using a Jasco J-710 spectropolarimeter with a thermostatically controlled compartment at 25 °C. For near-UV and visible wavelengths, the protein concentration varied from 1 to 2 mg/mL in a cuvette with a path length of 1 cm. Routinely, three spectra were recorded at a scan speed of 50 nm/min with a bandwidth of 2 nm and averaged automatically, except where indicated. For far-UV measurements, the protein concentration was 0.1 mg/mL with a path length of 0.1 cm.

pH Studies. The log $K_{d(PLP)}$, log k_{cat}, and log k_{cat}/K_m values for the wild type and mutant versus pH were fitted to the appropriate equations:

$$\log Y = \log \frac{C}{1 + \frac{H}{K_1}} \tag{2}$$

$$\log Y = \log \frac{C}{1 + \frac{H}{K_1} + \frac{K_2}{H}} \tag{3}$$

$$\log Y = \log \frac{Y_L + Y_H\left(\frac{H}{K_1}\right)}{1 + \frac{H}{K_1}} \tag{4}$$

where K_1 and K_2 represent the ionization constants for the enzyme and reactant functional group, respectively, Y is the value of the parameter observed at any pH, C is the pH-independent value of Y, H is the hydrogen ion concentration, and Y_L and Y_H are constant values of Y at low and high pH, respectively.

Absorbance data were fitted to eq 5 or 6:

$$A = \frac{A_1 - A_2}{1 + 10^{pH - pK_{spec}}} + A_2 \tag{5}$$

$$A = \frac{A_1 - A_2}{1 + 10^{pK_{spec} - pH}} + A_2 \tag{6}$$

where A_1 and A_2 are the higher and the lower absorbance limits at a particular wavelength, respectively.

Pre-Steady-State Kinetic Analysis by UV−Vis Stopped-Flow Spectroscopy. The wild type or Tyr 64 mutant (20 μM) was mixed using a Biologic SFM300 mixer with an equal volume of β-chloro-L-alanine in 20 mM Bis-Tris-propane (pH 7.4). Reactions proceed at 25 or 15 °C, and coenzyme absorbance changes were monitored with a TC10-100 (path length of 1 cm) quartz cell coupled to a BioKine PMS-60 instrument. The dead time was 3.6 ms at a flow velocity of 12 mL/s. Absorbance scans (500) from 300 to 550 nm were collected on a logarithmic time scale with a J&M Tidas 16 256 diode array detector (Molecular Kinetics, Pullman, WA). Data were analyzed using either SPECFIT (Spectrum Software Associates, Chapel Hill, NC) or Biokine 4.01 (Biologic, Claix, France) to determine the observed rate constants. Single-wavelength time courses were fit to an equation of the following general form:

$$A_t = A_\infty \pm \sum A_i \exp(-k_{obs} t) \tag{7}$$

where A_t is the absorbance at time t, A_i is the amplitude of each phase, k_{obs} is the observed rate constant for each phase, and A_∞ is the final absorbance.

Rapid Chemical Quench Studies. The chemical quench kinetic measurements were performed at 5 and 25 °C for the wild type and mutant, respectively, by mixing 70 μL portions of wild-type or mutant enzymes (~16 μM) and 70 μL portions of 20 mM β-chloro-L-alanine in 20 mM Bis-Tris-propane (pH 7.4). The reactions were quenched by mixing the solutions with an equal volume of 6 M perchloric acid in the quench syringe. Reaction times ranged from a minimum of 9 ms to 0.8 s. The amount of pyruvate in the solutions was determined by HPLC as described above. Pyruvate produced at different reaction times was plotted against time and fitted to eq 8 (*17*):

$$P_t = A(1 - e^{-k_b t}) + k_{ss} E_0 t \tag{8}$$

where P_t represents the product concentration at aging time t, A is the amplitude of the burst phase, k_b is the burst rate constant, k_{ss} is the steady-state rate constant, and E_0 is the total enzyme active site concentration.

All data analysis for determining model-derived kinetic parameters was performed by nonlinear curve fitting using KaleidaGraph 3.52 (Synergy Software, Reading, PA). In all cases, the best fit of the data was chosen on the basis of the lowest values of standard errors of the fitted parameters.

RESULTS

Spectroscopic Properties of the Y64A Mutant. Like wild-type cystalysin, the Tyr 64 mutant binds 2 mol of PLP per dimer. At pH 7.4, the wild type displays characteristic absorption and CD spectra with maxima at 418 and 320 nm, which can be attributed to the ketoenamine form of the Schiff base and a substituted aldamine, respectively (*2*). The absorption and CD spectra of the Tyr 64 mutant exhibit maxima at 412 and 325 nm. The relative intensities of the absorbance and the positive dichroic bands at 412 nm were significantly lower than those at 418 nm of the holoenzyme, while the intensities at 325 nm were higher than those at 320 nm of the holoenzyme (Figure 1A,B). With respect to the wild type, the mutant displays a decrease in the intensity of negative dichroic bands in the aromatic region of 288−296 nm and an increase in the intensity of the positive band at 275 nm. The circular dichroism spectra in the range of 190−240 nm of mutant and wild-type enzymes appear to be almost indistinguishable. Like the wild type, the mutant emits at 337 nm upon excitation at 280 nm (data not shown). Excitation at 412 nm of the Tyr 64 mutant shows an emission spectrum at 500 nm whose intensity is ~3-fold lower than that of the wild-type enzyme. It is of interest that upon

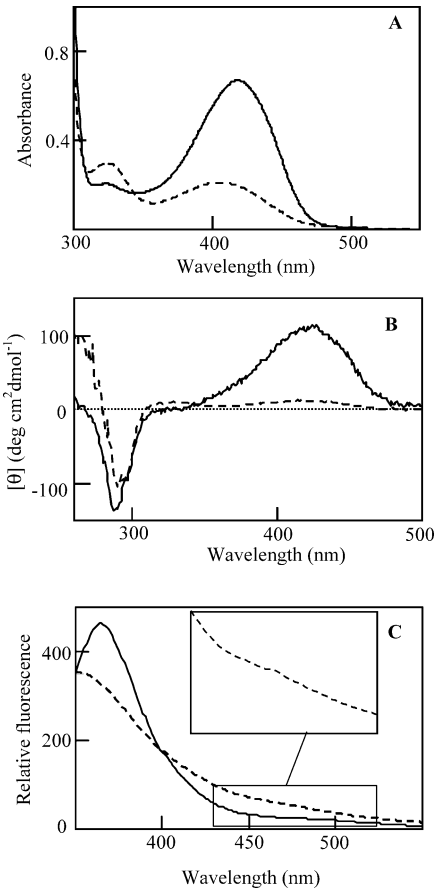

FIGURE 1: Absorption and CD spectra of the wild type and Tyr 64 mutant of cystalysin. (A) Absorption spectra of the wild type (—) and Tyr 64 mutant (– – –) in 20 mM Bis-Tris-propane (pH 7.4) at a concentration of 50 μM. (B) CD spectra. Symbols for the wild type and mutant are the same as those in panel A. (C) Fluorescence emission spectra upon excitation at 320 or 325 nm for the wild type (11 μM) or Tyr 64 mutant (50 μM), respectively. Symbols for the wild type and mutant are the same as those in panel A.

excitation at 320 nm the wild type exhibits a consistent emission at 367 nm (*2*), while upon excitation at 325 nm, the mutant displays a very faint emission at 450−460 nm (Figure 1C). Altogether, these data suggest that, although small conformational alterations may occur in the active site topography, no appreciable change in the secondary and tertiary structure occurs upon substitution of alanine for Tyr 64.

The Tyr 64 Mutation Weakens PLP Binding. Figure 2 shows that the apparent dissociation constant for PLP, $K_{d(PLP)}$, determined from the effect of the coenzyme concentration on the eliminase activity of the apoenzyme form of the wild type and Tyr 64 mutant increases as the pH increases. The pH dependence of $K_{d(PLP)}$ fits well to eq 4, giving p$K_{d(PLP)}$ values of 8.1 ± 0.1 and 7.83 ± 0.07 for the wild type and mutant, respectively (Table 1). The data of Figure 2 indicate that the extent to which the Tyr 64 to Ala substitution weakens PLP binding depends on pH. The apparent $K_{d(PLP)}$ for the Tyr 64 mutant is ~180-fold higher than that of the wild type at low pH, while it is ~5-fold higher at high pH. The measured $K_{d(PLP)}$ is an apparent dissociation constant because it is determined from activity in the presence of β-chloro-L-alanine. True $K_{d(PLP)}$ values for PLP binding to the apo form of wild-type and mutant enzymes have been determined by CD titration measurements. The results show

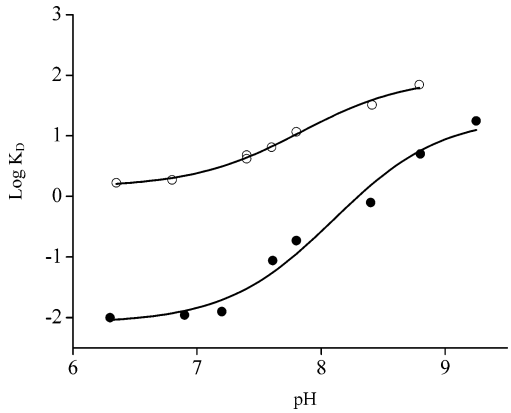

FIGURE 2: pH dependence of $K_{d(PLP)}$ of the wild type and Tyr 64 mutant. $K_{d(PLP)}$ values for the apo form of the wild type (10 nM) (●) and Tyr 64 mutant (0.4 μM) (○) were determined in 20 mM Bis-Tris-propane at the indicated pH by measuring pyruvate production in the presence of β-chloro-L-alanine at a saturating concentration and at varying concentrations of PLP. The points shown are the experimental values, while the curves are from fits to the data using eq 4.

that for either wild-type or mutant cystalysin the true $K_{d(PLP)}$ is slightly higher than the corresponding apparent $K_{d(PLP)}$ obtained from activity in the presence of β-chloro-L-alanine. The true $K_{d(PLP)}$ values for the wild type are $\ll$1 μM at pH 7 and 13 ± 2 μM at pH 9. For the mutant, the true $K_{d(PLP)}$ values have been found to be 17 ± 2, 21 ± 3, and 99 ± 12 μM at pH 7, 8, and 9, respectively. The finding that the apparent $K_{d(PLP)}$ values for both wild-type and mutant enzymes obtained from activity in the presence of β-chloro-L-alanine are lower than the true $K_{d(PLP)}$ values indicates that substrate does increase the affinity for PLP. It is possible that this effect is due to a substrate-induced conformational change. Previous spectroscopic studies have provided evidence of changes in the orientation of PLP and in the relative orientations of aromatic residue(s) and of the cofactor upon binding of the ligand to cystalysin (*2*).

The Tyr 64 Mutation Alters the pH Dependence of the Absorption Spectra of Cystalysin. In a previous work, the pH dependence of the absorbance and fluorescence titrations of the free wild-type cystalysin−PLP complex has been determined at an enzyme concentration of 4.6 μM (*2*). The results reported above indicate that the $K_{d(PLP)}$ value increases above a pK of ~8, ranging from values of 8 ± 0.8 nM at low pH to 20 ± 1.5 μM at high pH. Thus, we became aware that the spectrophotometric pH titrations have not been correctly carried out in that the enzyme concentration was not higher than the $K_{d(PLP)}$ over the entire pH range that was examined. This observation prompted a re-examination of the pH dependence of the wild-type absorbance titration at an enzyme concentration higher than $K_{d(PLP)}$ in the pH range of 5.9−9.4. As shown in Figure 3A, the effect of pH on the absorption spectra was essentially identical to that reported previously. The intensity of the 418 nm band decreases, while that of the 320 nm band increases with an increase in pH. However, in contrast with spectra previously recorded at 4.6 μM enzyme, spectra recorded at an enzyme concentration higher that $K_{d(PLP)}$ exhibit a clear isosbestic point at 351 nm (Figure 3A). The pK_{spec} of this transition is ~8.3 (inset of Figure 3A), and as previously proposed, it can be attributed to the ionization of an enzyme group shifting the equilibrium between the species absorbing at 418 and 320 nm, previously

Table 1: p*K* Values Associated with Wild-Type and Tyr 64 Mutant Cystalysin

	wild type				Y64A mutant			
	pK_a1	pK_a2	pK_a3	pH-independent limits	pK_a1	pK_a2	pK_a3	pH-independent limits
k_{cat}(α,β-elimination)[a]		7.8 ± 0.1		41 ± 2 s^{-1} at low pH 209 ± 3 s^{-1} at high pH		7.9 ± 0.2		4.0 ± 0.4 s^{-1} at low pH 17 ± 1 s^{-1} at high pH
k_{cat}/K_m(α,β-elimination)[a]	6.22 ± 0.07		8.93 ± 0.08	33.4 ± 2.6 mM^{-1} s^{-1}	6.18 ± 0.09		8.73 ± 0.08	4.51 ± 0.4 mM^{-1} s^{-1}
k_{cat}(racemization)[b]	6.29 ± 0.05			1.5 ± 0.1 s^{-1}	6.51 ± 0.04			0.36 ± 0.02 s^{-1}
k_{cat}/K_m(racemization)[b]	6.45 ± 0.04			0.067 ± 0.003 mM^{-1} s^{-1}	6.0 ± 0.1			0.019 ± 0.001 mM^{-1} s^{-1}
$K_{d(PLP)}$[c]		8.1 ± 0.1		8 ± 0.8 nM at low pH 20.0 ± 1.5 μM at high pH		7.83 ± 0.07		1.4 ± 0.4 at low pH 93 ± 3 at high pH
absorbance internal aldimine pH titration[d]		8.27 ± 0.05 at 418 nm			6.5 ± 0.1 at 412 nm			
		8.38 ± 0.07 at 320 nm			6.6 ± 0.2 at 325 nm			
absorbance quinonoid pH titration[e]	6.0 ± 0.1							

[a] Assay conditions: 50 nM wild type and 100 μM exogenous PLP or 0.2 μM Tyr 64 mutant and 400 μM exogenous PLP. [b] Assay conditions: 6 μM wild type and 100 μM exogenous PLP or 20 μM Tyr 64 mutant and 400 μM exogenous PLP. [c] Measurements were taken at 10 nM wild type or 400 nM mutant in the apo forms. [d] Coenzyme absorbance pH titration of 50 μM wild type and 50 μM mutant. [e] pH absorbance titration at 506 nm of the L-methionine−wild type complex. All the measurements were performed in 20 mM Bis-Tris-propane at 25 °C.

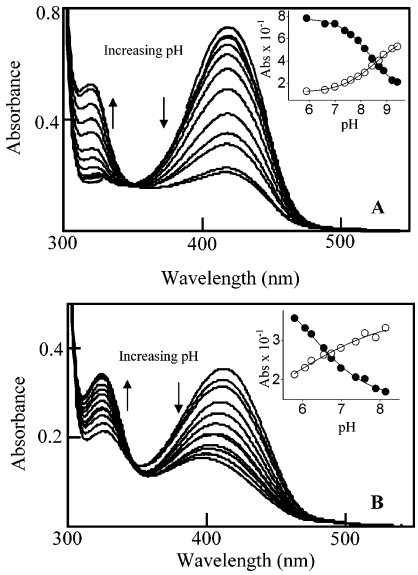

FIGURE 3: pH dependence of the UV−visible spectra of wild-type and Tyr 64 mutant cystalysin. (A) Spectra of the wild type (50 μM) were acquired in 20 mM Bis-Tris-propane at pH 5.90, 6.61, 6.99, 7.37, 7.61, 7.89, 8.15, 8.43, 8.70, 8.88, 9.21, and 9.41. The inset shows the pH dependence of the absorbance at 418 (●) and 320 nm (○). (B) Spectra of the Tyr 64 mutant (50 μM) were monitored in 20 mM Bis-Tris-propane at pH 5.8, 6.07, 6.23, 6.55, 6.75, 6.99, 7.37, 7.61, 7.89, 8.15, 8.41, and 8.70. The inset shows the pH dependence of the absorbance at 412 (●) and 325 nm (○). The solid lines represent the theoretical curves according to eqs 5 and 6.

attributed to a ketoenamine and a substituted aldamine, respectively (*2*). It has been suggested that a good candidate for an ionizing residue affecting this equilibrium in cystalysin could be Tyr 64. Variation of the absorbance spectra of the Tyr 64 mutant (50 μM) has been monitored as a function of pH. As shown in Figure 3B, the 412 nm absorbance decreases with an increase in pH with the concomitant increase in absorption at 325 nm. At pH >8, a blue shift of the 412 nm band could be observed which is possibly related to a small fraction of unbound PLP. Therefore, only the data at 412 and 325 nm ranging from pH 6 to 8 were considered for fitting a pK_{spec} value (eqs 5 and 6) (inset of Figure 3B). The pK_{spec} values obtained are 6.5 ± 0.1 and 6.6 ± 0.2 for the absorbance at 412 and 325 nm, respectively (Table 1). The same p*K* value has been obtained by measuring the decrease of the intensity of the 412 nm CD signal of the Tyr 64 mutant in the presence of saturating PLP concentrations (data not shown). Thus, mutation of Tyr 64 alters the pH dependence of the absorbance spectra of cystalysin.

The Tyr 64 Mutation Does Not Alter the pH Dependence of the Kinetic Parameters. In this work, the pH dependence of the kinetic parameters of wild-type and mutant enzymes for α,β-elimination of β-chloro-L-alanine and racemization of alanine has been measured at saturating concentrations of PLP. The results for α,β-elimination are reported in panels A and B of Figure 4. The log k_{cat}/K_m (obtained in the presence of exogenous PLP) decreases below p*K* values of 6.22 ± 0.07 and 6.18 ± 0.09 and above p*K* values of 8.93 ± 0.08 and 8.73 ± 0.08 for the wild type and Tyr 64 mutant, respectively. The pH-independent values of k_{cat}/K_m are 33.4 ± 2.6 and 4.51 ± 0.4 mM^{-1} s^{-1} for the wild type and Tyr 64 mutant, respectively (Table 1). The log k_{cat} profile for both wild-type and mutant enzymes increases from a constant value at low pH (41 ± 2 and 4.0 ± 0.4 s^{-1} for the wild type and mutant, respectively) to another constant value at high pH (209 ± 3 and 17 ± 1 s^{-1} for the wild type and mutant, respectively), giving pK_a values of 7.8 ± 0.1 and 7.9 ± 0.2 for the wild type and mutant, respectively (Table 1). Thus, the mutant retains 10% of the wild-type α,β-eliminase

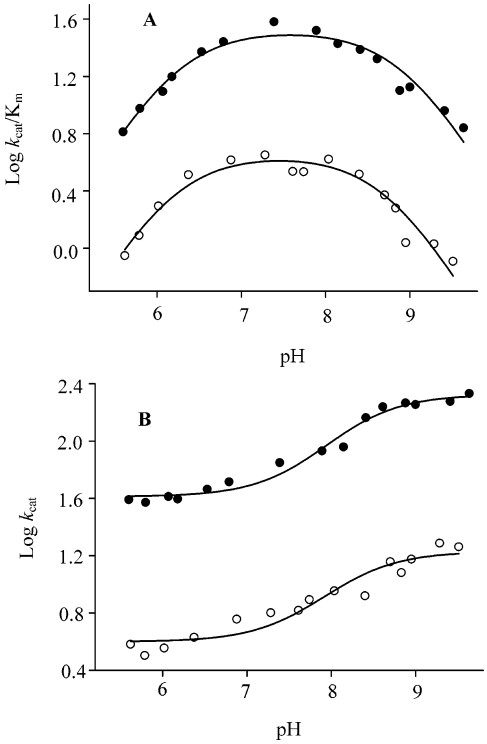

FIGURE 4: pH dependence of the kinetic parameters for α,β-eliminase activity of the wild type and Tyr 64 mutant with β-chloro-L-alanine. (A) Log k_{cat}/K_m profile and (B) log k_{cat} profile for the α,β-elimination reaction of the wild type (●) and Tyr 64 mutant (○) with β-chloro-L-alanine. The concentrations of the wild type and mutant are 50 and 400 nM, respectively. The assay were performed at 25 °C in 20 mM Bis-Tris-propane at the indicated pH in the presence of exogenous PLP at concentrations of 100 and 400 μM for the wild type and mutant, respectively. The points shown are the experimental values, while the curves are from fits to the data using eq 4 for log k_{cat} and eq 3 for log k_{cat}/K_m.

activity. For both wild-type and mutant enzymes, the log k_{cat} profile exhibits a partial change in eliminase activity as the pH is decreased below ~7.9, thus indicating that an enzyme group must be unprotonated for optimal activity. However, even when this group is protonated, the α,β-eliminase reaction proceeds at ~20% of the maximum rate observed above pH 8 for wild-type and mutant enzymes.

To establish if the ionizing group with a pK of ~6.3 observed in the k_{cat}/K_m profile is involved in the binding of substrate or catalysis, the pH dependence of the dissociation constants, K_D, of the wild type with glycine and L-methionine has been determined. Both glycine and L-methionine are unproductive substrate analogues, but while binding of glycine to wild-type cystalysin gives rise to an external aldimine absorbing at 429 nm, binding of L-methionine gives rise to an equilibrium mixture of external aldimine and quinonoid species (*2*). The fractional change (ΔA) in the absorbance at 429 or 506 nm as a function of glycine or L-methionine concentration, respectively, has been used to calculate the K_D and the ΔA_{max} for external aldimine and quinonoid species, respectively. As shown in Figure 5, the log K_D profiles for both the substrate analogues are pH-independent. This finding indicates that the group with a pK of ~6.2 present in the k_{cat}/K_m is not involved in binding of these substrate analogues. However, while the ΔA_{max} at 429 nm of the wild type−glycine complex is pH-independent, the ΔA_{max} at 429 and 506 nm of the wild type−L-methionine

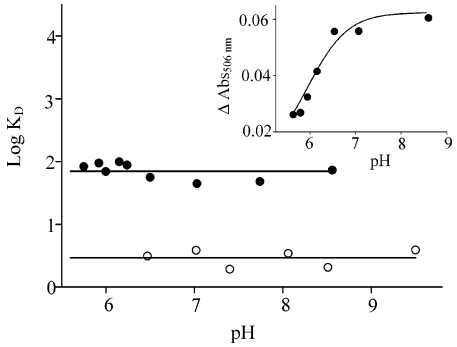

FIGURE 5: pH dependence of K_D of substrate analogues for wild-type cystalysin and of the absorbance at 506 nm of the L-methionine−wild type complex. K_D values for binding of glycine (●) and L-methionine (○) to wild-type cystalysin were determined in 20 mM Bis-Tris-propane at the indicated pH by measuring the fractional change in the absorbance at 429 or 506 nm as a function of glycine or L-methionine concentration, respectively. The lines represent the average value of K_D, equal to 2.9 ± 0.3 and 70 ± 2 mM for glycine and L-methionine, respectively. The inset shows the ΔA_{max} at 506 nm of the L-methionine−wild type complex as a function of pH. The points shown are the experimental values, while the curve is from a fit to the data using eq 6. The enzyme concentration was 5 μM.

complex exhibits a pH dependence consisting of a decrease in the 429 nm absorbance and an increase in the 506 nm absorbance with an increase in pH. The ΔA_{max} at 506 nm versus pH profile increases above a pK value of 6.0 ± 0.1 (inset of Figure 5) (Table 1). This value, roughly coincident with that observed in the k_{cat}/K_m profile, possibly reflects the ionization of a group responsible for abstraction of the proton at the α-carbon of the substrate. The pK of 8.7 observed in the k_{cat}/K_m profile likely reflects the pK of the substrate amino group (*2*).

The variation of the kinetic parameters for racemization of the wild-type and Tyr 64 mutant enzymes measured in the D → L direction is illustrated in panels A and B of Figure 6. All the measurements of racemase activity have been performed at saturating concentrations of PLP. The log k_{cat} and log k_{cat}/K_m profiles of the Tyr 64 mutant are qualitatively identical to the corresponding profiles for the wild type. The pK values derived from these profiles are reported in Table 1. The pH-independent value of k_{cat} for the mutant is 0.36 s^{-1}, ~17-fold lower than that of the wild type. Altogether, the results for the racemization reaction of both wild-type and mutant cystalysin indicate that a single ionizing group with a pK_a of 6−6.4 is involved in catalysis and must be unprotonated to achieve maximal velocity. The pH profiles for both the wild type and the Tyr 64 mutant measured in the L → D direction are essentially identical to those measured in the opposite direction (data not shown).

It should be noted that while the k_{cat}−pH profile for the α,β-elimination reaction catalyzed by the wild type is significantly different from that reported previously (pK of 6.6 in ref *2*), that derived here for racemization deviates slightly from that published previously (*3*). These results could be easily explained considering that previous kinetic data for α,β-elimination have been obtained in the absence of exogenous PLP at an enzyme concentration (50 nM) that is much lower than the $K_{d(PLP)}$ at high pH, whereas those for racemization were made at an enzyme concentration (6 μM) at least close to the $K_{d(PLP)}$ over the entire pH range that was examined.

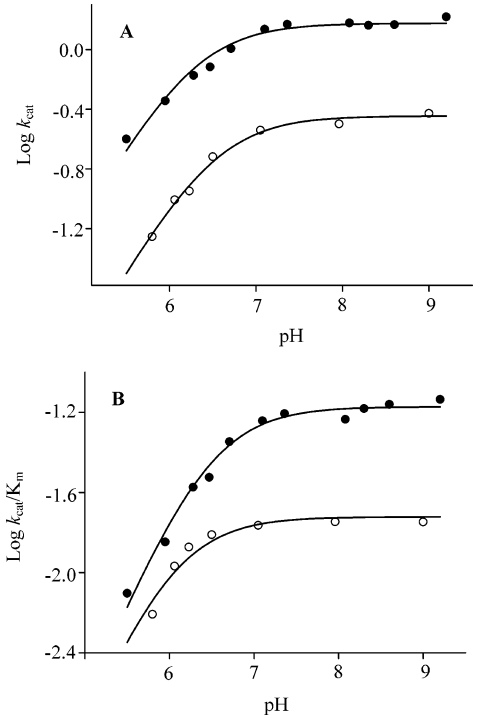

FIGURE 6: pH dependence of the kinetic parameters for racemase activity of the wild type and Tyr 64 mutant. (A) Log k_{cat} profile and (B) log k_{cat}/K_m profile for alanine racemase activity in the D → L direction of the wild type (●) and Tyr 64 mutant (○). The concentrations of the wild type and mutant are 6 and 20 μM, respectively. The assays were performed at 25 °C in 20 mM Bis-Tris-propane at the indicated pH in the presence of exogenous PLP at concentrations of 100 and 400 μM for the wild type and mutant, respectively. The points shown are the experimental values, while the curves are from fits to the data using eq 2 for both log k_{cat} and log k_{cat}/K_m.

The Tyr 64 mutant is able to catalyze transamination of L-alanine at a saturating concentration (500 mM) with an initial rate that is 40% of that of the wild type. On the other hand, the rate of transamination of D-alanine (500 mM) catalyzed by the mutant is ~1.4-fold higher than that catalyzed by the wild-type enzyme (data not shown).

The Tyr 64 Mutation Allows the Detection of the α*-Aminoacrylate Schiff Base.* As reported previously for wild-type cystalysin (*2*), the binding of L-serine to the Tyr 64 mutant leads to the appearance of an external aldimine absorbing at 429 nm. During the steady-state conditions, only an increase in the 330 nm region, due to the formation of pyruvate, is observed (data not shown). To obtain information about the identity of intermediates in the reaction of cystalysin with β-chloro-L-alanine and the rates of appearance and decomposition of these intermediates, we have carried out rapid-kinetic and steady-state spectroscopic studies. The rate of α,β-elimination of the wild-type enzyme toward β-chloro-L-alanine is so high (~60 s^{-1} at pH 7.4) that the reaction with this substrate cannot be followed by conventional spectroscopy. Only an increase at 330 nm due to pyruvate formation could be seen upon addition of this substrate to the enzyme. When rapid scanning stopped-flow measurements of this reaction were carried out at 25 °C, an immediate conversion of the 418 nm band into a 325 nm species could be observed, possibly due to the conversion of the internal aldimine to an external aldimine. This event is very fast and occurs within the dead time of the instrument (3.6 ms).

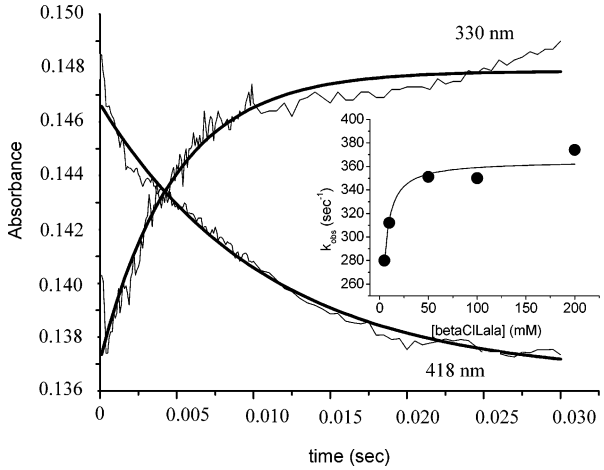

FIGURE 7: Single-wavelength stopped-flow measurements of the reaction of wild-type cystalysin with β-chloro-L-alanine at 15 °C. Reaction of wild-type cystalysin (10 μM) with β-chloro-L-alanine (10 mM) was carried out at 15 °C in 20 mM Bis-Tris-propane (pH 7.4). Time courses at 418 and 330 nm are reported. The solid lines are from a fit to eq 7. The inset shows the dependence of the k_{obs} for the decrease in the intensity of the 418 nm band as a function of β-chloro-L-alanine concentration. The points shown are the experimental values, while the curve is from a fit to the data using eq 9. The concentrations shown in parentheses are final concentrations after mixing.

Thereafter, the intensity of this band increases linearly with time which is consistent with pyruvate formation during the steady state. Thus, to slow the reaction of the wild type with β-chloro-L-alanine enough so that its kinetics could be measured, the experiment was repeated at 15 °C. As shown in Figure 7, upon addition of β-chloro-L-alanine to cystalysin, a decrease in the 418 nm absorbance with a concomitant increase in the 330 nm signal could be seen. The rate of formation of the external aldimine has been monitored by measuring the rate of disappearance of the 418 nm band as a function of substrate concentration. The apparent first-order rate constant, k_{obs}, shows a hyperbolic dependence on β-chloro-L-alanine concentration in the range of 10−200 mM (inset of Figure 7). The k_{obs} data were fitted to the following equation:

$$k_{obs} = k_{+2}\frac{[\beta\text{-chloro-L-alanine}]}{K_1 + [\beta\text{-chloro-L-alanine}]} + k_{-2} \qquad (9)$$

which describes the following two-step binding model assuming that the first step is rapid

$$\text{E} + \beta\text{-chloro-L-alanine} \overset{K_1}{\rightleftharpoons} \text{E}-\beta\text{-chloro-L-alanine intermediate} \overset{k_{-2}}{\underset{k_{+2}}{\rightleftharpoons}} \text{E}=\beta\text{-chloro-L-alanine Schiff base} \qquad (10)$$

where K_1 is the dissociation constant for the intermediate (Michaelis complex or geminal diamine) formed prior to the formation of the Schiff base species and k_{+2} and k_{-2} are first-order rate constants for the interconversion between the intermediate and the final Schiff base species. Estimated values of k_{+2}, k_{-2}, and K_1 based on the data in the inset of Figure 7 are 364 ± 76 s^{-1}, 10 ± 6 s^{-1}, and 7 ± 3 mM, respectively. The K_1 value is consistent with the K_m value (1.2 ± 0.1 mM) measured under steady-state conditions. It

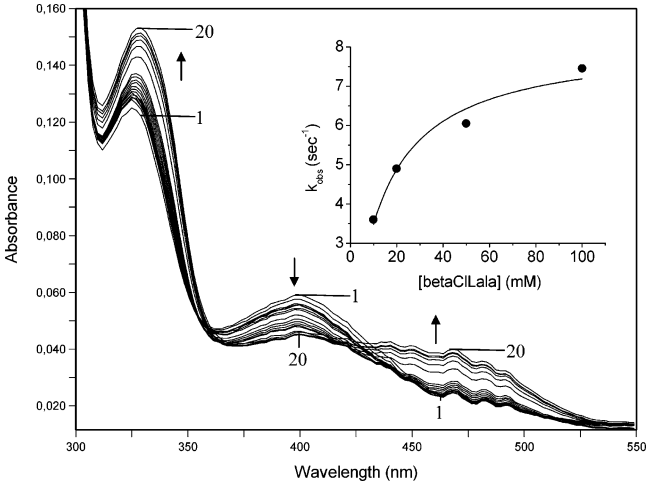

FIGURE 8: Rapid scanning stopped-flow spectra obtained upon reaction of Tyr 64 mutant cystalysin with β-chloro-L-alanine at 25 °C. Spectra 1−20 were collected at 0.009, 0.015, 0.030, 0.075, 0.090, 0.125, 0.150, 0.200, 0.245, 0.275, 0.425, 0.500, 0.575, 1.1, 1.85, 2.6, 3.35, 4.1, 4.85, and 5.60 s, respectively, upon mixing the Tyr 64 mutant (10 μM) with β-chloro-L-alanine (10 mM) in 20 mM Bis-Tris-propane (pH 7.4) at 25 °C. The inset shows the dependence of the k_{obs} for the increase in the 480 nm absorbance as a function of β-chloro-L-alanine concentration. The points shown are the experimental values, while the curve is from a fit to the data using eq 12.

follows that the rate of formation of the Schiff base at 25 °C can be estimated to be ~700−800 s^{-1} using the empirical rule of a 2-fold reduction in rate for a 10 °C reduction in temperature. This value is considerably higher than the k_{cat} value at 25 °C (~60 s^{-1}).

When β-chloro-L-alanine was added to the Tyr 64 mutant under steady-state conditions, in addition to an increase in the intensity of the 330 nm band, an absorbance band at ~480 nm, which can be attributed to an α-aminoacrylate intermediate, immediately appears. This species disappears with time, and a further increase at 330 nm, due to formation of pyruvate, can be seen. This is the first time in which the α-aminoacrylate species has been detected during the α,β-elimination catalyzed by cystalysin. To better assess the formation and decay of individual intermediates with greater precision, we carried out rapid scanning stopped-flow experiments (Figure 8). The spectra exhibit a rapid decrease in the intensity of the 412 nm band concomitant with the increase at 330 nm occurring in approximately 200−300 ms. This event is followed by formation of a 480 nm species which is complete within 5 s. The appearance of the aminoacrylate intermediate was monitored at 480 nm as a function of the substrate concentration. Time courses were analyzed with curve fitting software, and the k_{obs} value was determined. All curves were best fitted using a single exponential. A plot of the dependence of the k_{obs} on the concentration of β-chloro-L-alanine is shown in the inset of Figure 8. A mechanism of the type

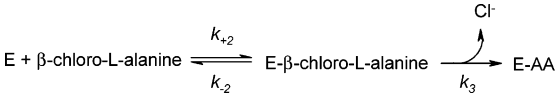

(11)

was used, where E is the free enzyme, E−β-chloro-L-alanine is the external aldimine, and E−AA is the α-aminoacrylate intermediate. The rate of formation of E−AA shows a

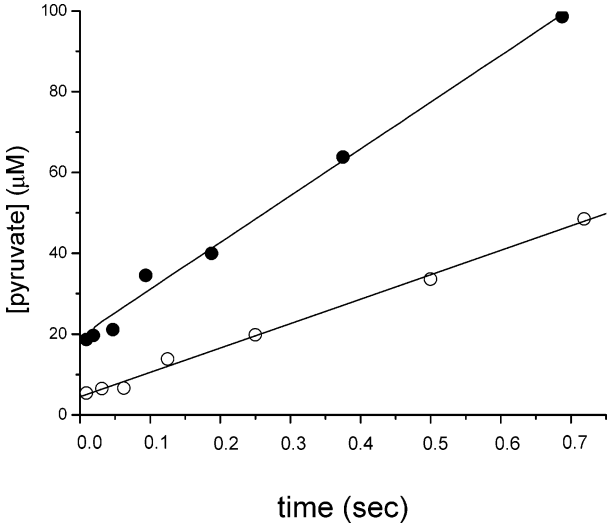

FIGURE 9: Chemical quench experiments of the wild type and Tyr 64 mutant with β-chloro-L-alanine. Kinetics of the pre-steady state of the wild type (8.1 μM) (●) and Tyr 64 mutant (8.37 μM) (○) with β-chloro-L-alanine (10 mM). Reactions were performed at 5 and 25 °C for the wild type and mutant, respectively, for the time shown on the *x*-axis, quenched with 2 M $HClO_4$, and the amount of pyruvate was measured by HPLC analysis. The points shown are the experimental values. The curve for the wild type represents the best fit to eq 8 with a burst amplitude of 19 ± 2 μM, a burst rate, k_b, of 223 ± 85 s^{-1}, and a steady-state rate, k_{ss}, of 13.8 ± 0.6 s^{-1}. The line shown for the mutant is a fit to the linear equation $y = ax + b$, where a = 60 ± 2 μM/s and b = 4.5 ± 0.6 μM. The concentrations shown in parentheses are final concentrations after mixing.

hyperbolic dependence on β-chloro-L-alanine concentration. This dependence indicates that the slow step in the reaction is the conversion of the external aldimine to E−AA. The k_{obs} is given by the equation

$$k_{obs} = \frac{k_3[\beta\text{-chloro-L-alanine}]}{K_2[\beta\text{-chloro-L-alanine}]} \qquad (12)$$

where $K_2 = k_{-2}/k_{+2}$. Fitting the data of the inset of Figure 8 to eq 12 gave a k_3 of 7.5 ± 0.1 s^{-1} and a K_2 of 8 ± 3 mM. It should be noted that the k_3 value is similar to the k_{cat} value of α,β-elimination catalyzed by the Tyr 64 mutant measured under steady-state conditions (6.7 s^{-1}).

The Tyr 64 Mutation Changes the Rate-Limiting Step of the α,β-Elimination Reaction. Rapid chemical quench experiments were performed to examine the pre-steady state of the α,β-elimination reaction of the wild-type and Tyr 64 mutant cystalysin with β-chloro-L-alanine. It was not possible to assess reliably the formation of pyruvate during the reaction catalyzed by the wild type, as the reaction occurs too rapidly and the initial burst could not be clearly defined. Thus, the reaction was performed at 5 °C, and the results are reported in Figure 9. A fit of the data to a simple linear equation gives a *y*-intercept value of 17.5 ± 0.8 μM and a slope of 116.3 ± 0.2 μM s^{-1}. Since the enzyme concentration after mixing was 8.1 μM, the value of k_{cat} taken from this experiment is 14.3 s^{-1}, in agreement with the k_{cat} of 11.2 ± 0.1 s^{-1} obtained in steady-state kinetic measurements at 5 °C. Considering the fact that the enzyme active site concentration in rapid chemical quench experiments is 16 μM, the initial lag could be interpreted in terms of a burst. As

shown in Figure 9, a satisfactory fit of the data was obtained using eq 8. The first turnover occurred at a rate, k_b, of 223 ± 85 s^{-1} with an amplitude of 1/enzyme active site concentration, whereas subsequent turnovers were at a rate, k_{ss}, of 13.8 ± 0.6 s^{-1}, in agreement with the independently determined steady-state rate (k_{cat} = 11.2 s^{-1}). Unfortunately, we were not able to determine the building up of the burst phase, given the high rate of the reaction. Thus, it is reasonable to postulate that the rate-limiting step of the α,β-elimination reaction catalyzed by wild-type cystalysin occurs after the chemical step, and could be assigned to product release.

Chemical quench experiments of the Tyr 64 mutant with β-chloro-L-alanine at a saturating concentration were carried out at 25 °C. The best fit of the data reported in Figure 9 is to a simple linear equation, and we are not able to obtain an adequate fit of the data to an exponential equation with either a burst (eq 8) or a lag. The slope of the line in Figure 9 is 60 ± 2 μM s^{-1}, and the enzyme concentration after mixing was 8.37 μM; therefore, the value of k_{cat} taken from this experiment is 7.1 s^{-1}, in good agreement with the k_{cat} of 6.7 s^{-1} obtained in steady-state kinetic measurements. The *y*-intercept extrapolates to a value of 4.5 ± 0.6 μM which corresponds to only 0.25 per enzyme active site, thus arguing against the presence of a burst phase. Altogether, the rapid chemical quench experiments support the view that, unlike for the wild-type enzyme, the product release is not the rate-limiting step for the Tyr 64 mutant.

DISCUSSION

The finding that the substitution of Tyr 64 of *T. denticola* cystalysin with alanine apparently causes at pH 7.4 an ~100-fold decrease in PLP binding affinity provides evidence that Tyr 64 plays a role in cofactor binding. This functional role is consistent with the crystallographic evidence that this residue interacts with the PLP phosphate (*7*) and emphasizes the remarkable relevance of the noncovalent interaction between the phosphate of PLP and Tyr 64. Nevertheless, it should be noted that PLP binds to either wild-type or mutant cystalysin with an affinity at alkaline pH values lower than that at acidic pH values. More will be said below about this pH dependence.

In addition, our results show that mutation of Tyr 64 alters the pH dependence of the absorption spectra of cystalysin. One ionization was observed in the cystalysin−PLP coenzyme absorbance spectra for both the wild type and mutant taken as a function of pH. This ionization has pK_{spec} values of ~8.3 and 6.5 for the wild type and mutant, respectively. It was suggested that the pK_{spec} could reflect either the ionization of an enzyme group directly involved in the formation of the substituted aldamine or another enzyme group whose ionization would influence the equilibrium between the species absorbing at 418 and 320 nm (*2*). The same equilibrium cannot be suggested for the Tyr 64 mutant. On the basis of studies on model systems of Schiff bases of PLP with amines in various solvents (*20*, *21*), the ~450−460 nm fluorescence from the Tyr 64 mutant is consistent with the assignment of an enolimine structure for the 325 nm absorption band of the Tyr 64 mutant. Taken together, these results suggest that mutation of Tyr 64 (i) does not affect the global conformation of cystalysin but does affect the environment of the PLP cofactor as reflected by the change in the form of the internal aldimine and (ii) impairs the formation of the substituted aldamine present in the wild-type cystalysin. The latter observation strongly supports the view that Tyr 64 (or a water molecule held in place by Tyr 64) is the residue involved in the nucleophilic attack on C4′ of the coenzyme in the internal aldimine. It would be interesting to check if a tyrosyl residue is also implicated in the substituted aldamine present in tryptophanase (*22*, *23*) and 5-aminolevulinate synthase (*24*).

Steady-state kinetic studies of α,β-elimination reaction and of alanine racemase activity catalyzed by the wild type and Tyr 64 mutant indicate that Tyr 64 is not an essential residue for catalysis. Mutation of Tyr 64 results in a 70−90% reduction in k_{cat} and k_{cat}/K_m values for eliminase and racemase activities. A similar reduction in transaminase activity toward L-alanine could be observed. On the other hand, the Tyr 64 mutant is able to catalyze the transamination of D-alanine with a rate 1.4-fold higher than that of the wild type. The three-dimensional structure of cystalysin complexed with L-aminoethoxyvinylglycine (*2*) reveals an interaction between Tyr 64 and Lys 238, both located on the *si* face of the cofactor. This could explain the reason for the decrease in the Tyr 64 mutant of all activities (α,β-elimination, racemization, and L-alanine transamination) involving Lys 238 as the acid−base catalyst. Therefore, it is not surprising that mutation of Tyr 64 does not alter, or even increases, the transamination of D-alanine, an event occurring through an acid−base catalyst on the *re* face (*6*). Despite the lower turnover numbers of α,β-elimination and racemization of the mutant in relation to those of the wild type, the pH−rate profiles for their reactions are very similar. Thus, none of the p*K*s observed for the wild-type enzyme reflects the ionization of the hydroxyl of Tyr 64. Moreover, mutation of Tyr to Ala does not significantly affect p*K* values of the active site, suggesting that the mutation does not have a disruptive effect on the active site structure.

A catalytic mechanism for the α,β-elimination and racemization (Scheme 1) has been proposed (*3*, *7*). The pH dependence of the k_{cat}/K_m of α,β-elimination and racemization and the k_{cat} of racemization and quinonoid absorbance titration together with previous kinetic studies of Lys 238 mutants (*5*) allow the assignment of the ionization of the group with a p*K* of 6−6.4 to the acid−base catalyst Lys 238 which could be responsible for abstraction of the proton at the α-carbon of the substrate. α,β-Elimination and racemization could share the step leading to the quinonoid intermediate, and the same catalytic residue is probably used in both reactions. What is the identity of the group with a p*K* of ~8 that only affects the k_{cat} for α,β-elimination catalyzed by both the wild type and mutant? It is likely the same one seen in the pH profile for $K_{d(PLP)}$ for wild-type and mutant enzymes. Its presence in the pH profile for $K_{d(PLP)}$ could suggest that the phosphate ester of the coenzyme is a likely origin of this pK_a, although its value is higher than that observed for the coenzyme phosphate group in D-serine dehydratase (*25*) and dialkylglycine decarboxylase (*26*). Following this view, the finding that the $K_{d(PLP)}$ value increases ~2500- and ~66-fold from low to high pH for the wild type and mutant, respectively, would indicate that the ionization of the coenzyme phosphate group affects the affinity of the coenzyme for the wild type more remarkably

Scheme 1: Proposed Catalytic Mechanism for the α,β-Elimination and Racemization Catalyzed by Cystalysin

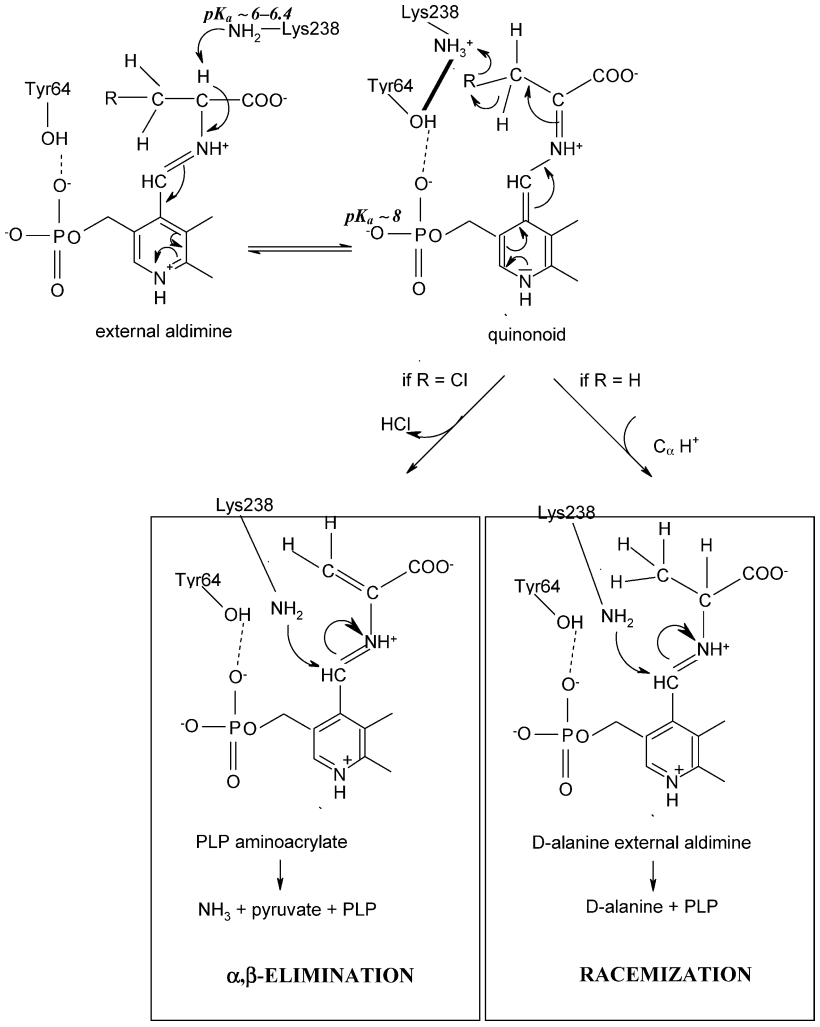

than that to the mutant. The relevant effect of this ionization in the wild type could be ascribed to the loss of the hydrogen bond between the hydroxyl group of Tyr 64 and the coenzyme phosphate group oxygen. At pH >8, the prevailing phosphate dianion form of PLP could be engaged in charge−charge electrostatic repulsion with the leaving group of the substrate during α,β-elimination. This could explain why a p*K* of ∼8 controls the k_{cat} of α,β-elimination but not that of racemization. Although this assignment should be taken with caution due to the tenuous nature of the evidence supporting it, it is consistent with the finding that the k_{cat} in pH profiles for α,β-elimination of both the wild type and mutant differs by a factor of only 4−5 at low and high pH. This means that the eliminase reaction is not absolutely dependent on the group that exhibits a p*K* value of ∼8, although this group can influence the chemistry of the reaction. It could also be possible that the p*K* observed in the $K_{d(PLP)}$ profile does not coincide with the p*K* of the k_{cat} profile. In this case, the group whose p*K* is present on the k_{cat} profile could be even remote from the active site and the effect on eliminase activity could be transmitted through the protein by a conformational change resulting in a conversion from a less to a more catalytically competent conformation form as the pH increases above 8. This interpretation is in line with the increase in k_{cat} for α,β-elimination at pH >8 for both wild-type and mutant enzymes but not with the k_{cat}−pH profile for racemization.

Virtually nothing is known about the location and amount of limitation of rate-determining steps along the reaction of α,β-elimination catalyzed by cystalysin. This kinetic analysis provided a quantitative description of the overall cystalysin reaction pathway and has highlighted the mechanistic role of Tyr 64. As a first event, upon substrate addition, a rapid conversion of the internal aldimine into a 330 nm absorbing species could be observed. Structures which could account for the absorbance in the 330 nm region could be the enolimine tautomer of external aldimine, the geminal diamine, and the enolimine tautomer of the α-aminoacrylate, all absorbing in the 320−350 nm range. However, the geminal diamine is the most unlikely candidate since it is quite unstable and weakly absorbing, and the enolimine tautomer of α-aminoacrylate could be ruled out considering that it appears earlier than the 480 nm band. All these considerations are consistent with the assignment of the 330 nm form to an external aldimine.

The finding that the α-aminoacrylate intermediate is detected in the reaction catalyzed by the Tyr 64 mutant and not in the reaction catalyzed by the wild type provides evidence that tyrosine to alanine mutation significantly alters the step mainly associated with aminoacrylate formation, i.e., the release of the leaving group. Additionally, rapid chemical quench studies of the mutant, showing that the rate of linear production of pyruvate is similar to that of aminoacrylate formation and to that of the steady-state k_{cat}, support the view

that the formation of the α-aminoacrylate in the mutant is the rate-determining step. On the other hand, the results of quenching analysis of wild-type cystalysin show a burst of pyruvate, thus indicating that the rate-determining step is most likely associated with the release of the product. It can be argued that mutation of Tyr 64 results in a change in the rate-limiting step of α,*β*-elimination.

Krupka et al. (*7*) proposed that for the C*β*−R bond cleavage in the α,*β*-elimination of cystalysin the positively charged amino group of Lys 238 is guided toward the leaving group (R) by interaction with Tyr 64. According to this view, Tyr 64 during the catalytic cycle acts by positioning the Lys *ϵ*-amino group in a proper orientation for catalysis. This is in agreement with the detection of the aminoacrylate intermediate with the mutant. The reduced turnover rate implies that the loss of Tyr 64 may slow the formation of this species. It can be reasonably suggested that the correct positioning of protonated Lys 238 mediated by Tyr 64 could also be an important requirement for Cα protonation in racemization and for C4′ protonation in transamination of L-alanine. This is consistent with the findings that the Tyr 64 mutant exhibits a remarkable reduction of both racemase and L-alanine transaminase activities and retains its full D-alanine transaminase activity.

In conclusion, our data demonstrate that Tyr 64, besides contributing remarkably to the PLP binding, appears to be implicated in the nucleophilic attack on C4′ of the coenzyme in the internal aldimine. It also emerges that, although Tyr 64 is not an essential residue for α,*β*-eliminase and racemase activities, it plays an important role in properly orienting Lys 238 to facilitate catalysis. Moreover, stopped flow coupled to quench-flow analyses of the reaction of the wild type and Y64A mutant with *β*-chloro-L-alanine permit us to substantiate the presence of the α-aminoacrylate species as an intermediate in the α,*β*-elimination catalyzed by cystalysin and to establish that pyruvate release is the rate-limiting step in the catalytic pathway.

REFERENCES

1. Chu, L., Burgum, A., Kolodrubetz, D., and Holt, S. C. (1995) The 46-Kilodalton-hemolysin gene from *Treponema denticola* encodes a novel hemolysin homologous to aminotransferases, *Infect. Immun. 63*, 4448−4455.
2. Bertoldi, M., Cellini, B., Clausen, T., and Borri Voltattorni, C. (2002) Spectroscopic and kinetic analyses reveal the pyridoxal 5′-phosphate binding mode and the catalytic features of *Treponema denticola* cystalysin, *Biochemistry 41*, 9153−9164.
3. Bertoldi, M., Cellini, B., Paiardini, A., Di Salvo, M., and Borri Voltattorni, C. (2003) *Treponema denticola* cystalysin exhibits significant alanine racemase activity accompanied by transamination: Mechanistic implications, *Biochem. J. 371*, 473−483.
4. Cellini, B., Bertoldi, M., and Borri Voltattorni, C. (2003) *Treponema denticola* cystalysin catalyzes *β*-desulfination of L-cysteine sulfinic acid and *β*-decarboxylation of L-aspartate and oxalacetate, *FEBS Lett. 554*, 306−310.
5. Bertoldi, M., Cellini, B., D'Aguanno, S., and Borri Voltattorni, C. (2003) Lysine 238 is an essential residue for α,*β*-elimination catalyzed by *Treponema denticola* cystalysin, *J. Biol. Chem. 278*, 37336−37343.
6. Cellini, B., Bertoldi, M., Paiardini, A., D'Aguanno, S., and Borri Voltattorni, C. (2004) Site-directed mutagenesis provides insight into racemization and transamination of alanine catalyzed by *Treponema denticola* cystalysin, *J. Biol. Chem. 279*, 36898−36905.
7. Krupka, H. L., Huber, R., Holt, S. C., and Clausen, T. (2000) Crystal structure of cystalysin from *Treponema denticola*: A pyridoxal 5′-phosphate-dependent protein acting as a haemolytic enzyme, *EMBO J. 19*, 3168−3178.
8. Grishin, N. V., Phillips, M. A., and Goldsmith, E. J. (1995) Modeling of the spatial structure of eukaryotic ornithine decarboxylases, *Protein Sci. 4*, 1291−1304.
9. Toney, M. D., and Kirsch, J. F. (1987) Tyrosine 70 increases the coenzyme affinity of aspartate aminotransferase. A site-directed mutagenesis study, *J. Biol. Chem. 262*, 12403−12405.
10. Toney, M. D., and Kirsch, J. F. (1991) Tyrosine 70 fine-tunes the catalytic efficiency of aspartate aminotransferase, *Biochemistry 30*, 7456−7461.
11. Chen, H.-Y., Demidkina, T. V., and Phillips, R. S. (1995) Site-directed mutagenesis of tyrosine 71 to phenylalanine in *Citrobacter freundii* tyrosine phenol-lyase: Evidence for dual roles of tyrosine 71 as a general acid catalyst in the reaction mechanism and in cofactor binding, *Biochemistry 34*, 12276−12283.
12. Clausen, T., Huber, T., Laber, B., Pohlenz, H.-D., and Messrschmidt, A. (1996) Crystal structure of the pyridoxal 5′-phosphate dependent cystathionine *β*-lyase from *Escherichia coli* at 1.83 Å, *J. Mol. Biol. 262*, 202−224.
13. Isupov, M. N., Antson, A. A., Dodson, E. J., Dodson, G. G., Dementieva, I. S., Zakomirdina, L. D., Wilson, K. S., Danter, Z., Lebedev, A. A., and Harutyunyan, E. H. (1998) Crystal structure of tryptophanase, *J. Mol. Biol. 276*, 603−623.
14. Clausen, T., Schlegel, A., Peist, R., Schneider, E., Steegborn, C., Chang, Y. S., Haase, A., Bourenkov, G. P., Bartunik, H. D., and Boos, W. (2000) X-ray structure of MalY from *Escherichia coli*, a pyridoxal 5′-phosphate-dependent enzyme acting as a modulator in mal gene expression, *EMBO J. 19*, 831−842.
15. Peterson, E. A., and Sober, H. A. (1954) Preparation of crystalline phosphorylated derivatives of vitamin B_6, *J. Am. Chem. Soc. 76*, 169−175.
16. Neidle, A., and Dunlop, D. S. (2002) Allosteric regulation of mouse brain serine racemase, *Neurochem. Res. 27*, 1719−1724.
17. Johnson, K. A. (1992) Transient state kinetic analysis of enzyme reaction pathways, *Enzymes 20*, 1−61.
18. Marceau, M., Lewis, S. D., Kojiro, C. L., Mountjoy, K., and Sharper, J. A. (1990) Disruption of active site interactions with pyridoxal 5′-phosphate and substrates by conservative replacements in the glycine rich loop of *Escherichia coli* D-serine dehydratase, *J. Biol. Chem. 265*, 20421−20429.
19. Gong, J., Kay, C. J., Barber, M. J., and Ferreira, G. C. (1996) Mutations at a glycine loop in aminolevulinate synthase affect pyridoxal phosphate cofactor binding and catalysis, *Biochemistry 35*, 14109−14117.
20. Honikel, K. O., and Madsen, N. B. (1972) Comparison of the absorbance spectra and fluorescence behaviour of phosphorylase b with that of model pyridoxal phosphate derivatives in various solvents, *J. Biol. Chem. 247*, 1057−1064.
21. Vazquez Segura, M. A., Donoso, J., Munoz, F., Blanco, F. G., Del Vado, M. A. G., and Echevarria, G. (1994) Photophysical study of the Schiff bases of 5′-deoxypyridoxal and *n*-hexylamine in cationic micelles, *Photochem. Photobiol. 60*, 399−404.
22. Morino, Y., and Snell, E. E. (1967) The relation of spectral changes and tritium exchange reactions to the mechanism of tryptophanase-catalyzed reactions, *J. Biol. Chem. 242*, 2800−2809.
23. Ikushiro, H., Hayashi, H., Kawata, Y., and Kagamiyama, H. (1998) Analysis of the pH-and ligand-induced spectral transitions of tryptophanase: Activation of the coenzyme at the early steps of the catalytic cycle, *Biochemistry 37*, 3043−3052.
24. Zhang, J., Cheltsov, A. V., and Ferreira, G. C. (2005) Conversion of 5-aminolevulinate synthase into a more active enzyme by linking the two subunits: Spectroscopic and kinetic properties, *Protein Sci. 14*, 1190−1200.
25. Schnackerz, K. D., Feldman, K., and Hull, W. E. (1979) Phosphorus-31 nuclear magnetic resonance study of D-serine dehydratase: Pyridoxal phosphate binding site, *Biochemistry 18*, 1536−1539.
26. Zhou, X., and Toney, M. D. (1999) pH studies on the mechanism of the pyridoxal phosphate-dependent dialkylglycine decarboxylase, *Biochemistry 38*, 311−320.

BI051433N